

# Simultaneous clock recovery and demultiplexing of a 320 Gb/s OTDM system using an optoelectronic oscillator based on cascaded MZM and PolM

Yu Ji (嵇 蓉), Xixue Jia (贾锡学), Yan Li (李 岩)\*, Jian Wu (伍 剑), and Jintong Lin (林金桐)

State Key Laboratory of Information Photonics and Optical Communications,  
Beijing University of Posts and Telecommunications, Beijing 100876, China

\*Corresponding author: liyan1980@bupt.edu.cn

Received December 19, 2012; accepted January 25, 2013; posted online April 19, 2013

An improved optoelectronic oscillator scheme for an optical time division multiplexing (OTDM) system based on cascaded Mach-Zehnder modulator (MZM) and polarization modulator (PolM) is experimentally investigated. The system can simultaneously realize clock recovery and demultiplexing. With the MZM working at peak point to generate return-to-zero-33 optical pulses and the PolM working as an equivalent intensity modulator, a high-quality clock signal with 35-fs timing jitter is extracted from the 160-GBaud OTDM-differential quaternary phase-shift keying signal. Narrow short optical switch gates (4 ps) are also generated to demultiplex 160-GBaud signals to 40-GBaud signals. Error-free performance is achieved with 2.4-dB power penalty in the worst case.

OCIS codes: 060.2330, 130.4110.

doi: 10.3788/COL201311.050602.

Optical time division multiplexing (OTDM) is a promising technique for overcoming the bottleneck of electronic bandwidth. Ultrahigh-speed OTDM systems operating at speeds of up to terabits per second have been successfully demonstrated<sup>[1,2]</sup>. Therefore, considerable challenges regarding clock recovery and optical demultiplexing module at the receiver side have been raised. Given that the recovered clock is used to demultiplex a high-speed OTDM signal to relatively low speed tributary signals, the quality of the recovered clock affects the stability of the tributary signals and the overall performance.

Clock recovery and demultiplexing are widely studied through various approaches. In recent years, all-optical clock recovery schemes such as semiconductor optical amplifier-based<sup>[3]</sup> and self-pulsated distributed feedback<sup>[4]</sup> lasers have been studied to determine all-optical clock recovery and overcome the problem of limited electronic bandwidth. However, all-optical clock recovery schemes are unstable and poorly qualified compared with optoelectronic oscillator (OEO) schemes based on a Mach-Zehnder modulator (MZM)<sup>[5]</sup>. Demultiplexing is another key technique for realizing an interface between a high-speed optical signal and a relatively low base-rate signal. Various schemes based on electro-optical modulators and nonlinear optical components have been proposed. Nonlinear effects such as four-wave mixing<sup>[6]</sup> and cross-phase modulation<sup>[7]</sup>, are also used to generate a high-speed optical gate. However, these schemes are low quality and expensive. Modulator-based demultiplexing schemes including MZM<sup>[8]</sup>, electro-absorption modulator (EAM)<sup>[9]</sup>, and polarization modulator (PolM)<sup>[10]</sup> have a simple structure and stabilized operation. However, the insertion loss of an EAM is high, which degrades the signal-to-noise ratio (SNR) and requires temperature feedback control.

In this letter, we demonstrate an OEO based on cascaded MZM and PolM to realize clock recovery and demultiplexing simultaneously. The two cascaded mod-

ulators can enhance clock tone and generate a short-pulse window. The timing jitter of the 40-GHz recovered clock is about 35 fs, and the full-width at half-maximum (FWHM) of the switch gate is 4 ps. This scheme has the advantages of low insertion loss compared with EAM as well as simple structure and low cost compared with all-optical schemes.

The main principle of our proposed improved OEO scheme is similar to the traditional OEO<sup>[11-13]</sup>. It is a positive feedback loop consisting of a MZM, a PolM, an optical fiber, a photodetector (PD), a bandpass filter (BPF), and a radio-frequency amplifier. A long fiber is used for time delay and energy storage to realize a high  $Q$  factor. OTDM clock recovery is based on OEO prescaled injection locking. OEO free running frequency is locked to the prescaled OTDM clock signal, which enables tributary clock recovery to be realized. Meanwhile, the base-rate tributary is demultiplexed from incoming high-speed OTDM signals from the other part of the polarization beam splitter (PBS) based on the optical switch window generated from the cascaded MZM and PolM.

The narrow pulse switch gate generated by the cascaded MZM and PolM is investigated. Figure 1 shows the scheme and principle of the optical pulse window generation.

The output of MZM intensity modulation can be expressed as

$$T = \cos^2 \left\{ \frac{\pi}{2V_\pi} [V(t) + V_B] \right\} \\ = \frac{1}{2} \left\{ 1 + \cos \left\{ \frac{\pi}{V_\pi} [V(t) + V_B] \right\} \right\}. \quad (1)$$

When  $V_B=0$ ,  $2V_\pi$ ,  $4V_\pi, \dots$ , MZM works at the maximum transmittance point and generates return-to-zero (RZ)-33 narrow gates (solid line in Fig. 2(a)).

PolM is a phase modulator that supports both transverse electric (TE) and transverse magnetic (TM) modes but with opposite phase modulation indices. The optical

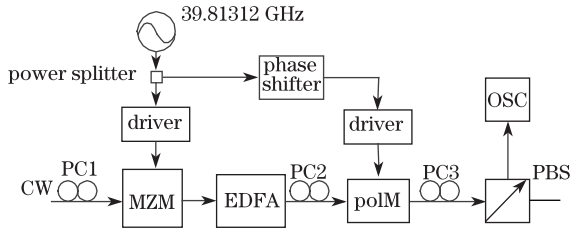


Fig. 1. Scheme and principle of the optical pulse window generation.

field at the output of the PolM along the two principal axes can be expressed as<sup>[11]</sup>

$$\begin{bmatrix} E_x \\ E_y \end{bmatrix} = \sqrt{\alpha} E_{in} \begin{bmatrix} \exp\left(\frac{1}{2}\beta \sin \omega_0 t\right) \\ \exp\left(-\frac{1}{2}\beta \sin \omega_0 t\right) \end{bmatrix}, \quad (2)$$

where  $\alpha$  is the transmission factor,  $\beta$  is the phase modulation index, and  $\omega_0$  is the angular frequency of OEO oscillation. The PolM we used contains a built-in  $45^\circ$  polarizer that allows the optical signal to be equally distributed to the two principal axes and becomes two modulated signals. By applying a polarization controller (PC) along with a PBS to the two signals with the principal axis of the PBS aligned  $45^\circ$  to one principal axis of the PolM, we can obtain the field expression at the output of the PBS:

$$E_0 \frac{\sqrt{2}}{2} (E_x + E_y \cdot e^{-j\phi_B}), \quad (3)$$

where  $\phi_B$  is the static phase item introduced by the PC placed before the PBS. Thus, the output optical power can be expressed as

$$E_{out} = |E_{out}|^2 = \alpha E_{in}^2 [1 + \cos(\beta \sin \omega_0 t + \phi_B)]. \quad (4)$$

We can easily obtain the optical intensity transfer function by dividing  $P_{out}$  by  $P_{in}$

$$T = \frac{P_{out}}{E_{in}} = \alpha [1 + \cos(\beta \sin \omega_0 t + \phi_B)]. \quad (5)$$

The transfer function is equivalent to that of a MZM, which is biased at a minimum transmission point when  $\phi_B = \pi$  or at a quadrature transmission point when  $\phi_B = -\frac{\pi}{2}$ . When we cascade MZM with PolM, MZM is biased at a maximum transmission point  $\phi_B = -\frac{\pi}{2}$  by tuning the PC placed after PolM, and a narrow pulse gate can be generated as shown in Fig. 2(b).

Figure 3 shows the improved OEO experimental setup. The MZM is driven by a 40-GHz sinusoidal clock from a low-phase-noise signal synthesizer (Agilent E8257D) with a peak-to-peak voltage of approximately 14 V (equal to the  $2V_\pi$  of MZM-a at 40 GHz). The direct current (DC) is biased at the peak point to generate 80-GHz RZ-33 signals with a FWHM of 4 ps. The PolM uses a commercial 40-GHz PolM device (Versawave PL-40G-5-1550). The 3-dB band width of the PolM is 40 GHz, and the  $V_\pi$  is approximately 5 V at 40 GHz. The voltage applied to PolM is 18 dBm ( $V_{peak}$  to peak). PolM functions as an equivalent MZM biased at a quadrature transmission point. The output of the two cascaded modulators is

initially characterized for CW input at 1553.9-nm wavelength. The generated 40 GHz pulse train is measured by a 500-GHz optical sampling oscilloscope (OSO; EXFO-PSO-102).

The 40-GHz clock signal is extracted using the improved OEO feedback loop. This feedback loop consists of a 50-GHz PD with a responsivity of 0.65 for optical to electrical conversion, a low noise amplifier with a noise figure less than 4 dB and a small signal gain of 48 dB, a BPF with a 3 dB bandwidth of 20 MHz and out-of-band suppression larger than 50 dB, a power amplifier with saturation output power of 27 dBm, a power splitter, as well as a phase shifter to adjust the feedback clock signal (Fig. 3).

The 160-GBaud differential quaternary phase-shift keying (DQPSK) clock recovery and demultiplexing performance of the proposed OEO are measured using the setup in Fig. 4. Short pulses with FWHM = 1.9 ps generated from the cascaded EAM and two-phase modulators are modulated with a  $2^7-1$  pseudorandom binary sequence (PRBS) data in an I/Q modulator, and DQPSK signals are created. The two output data from a 40-Gb/s pattern generator are de-correlated by a 63-bit time delay and amplified to 21 dBm (about  $2V_\pi$  at 40 GHz)

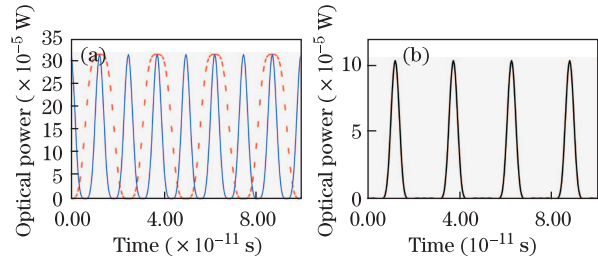


Fig. 2. Simulation results of the pulse window generation from the output of (a) MZM and (b) PolM.

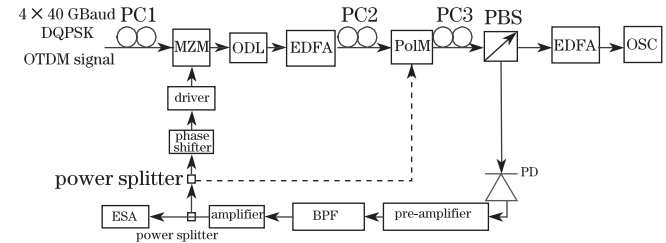


Fig. 3. Scheme and principle of the proposed improved OEO. ODL: optical delay line; ESA: electrical spectrum analyzer.

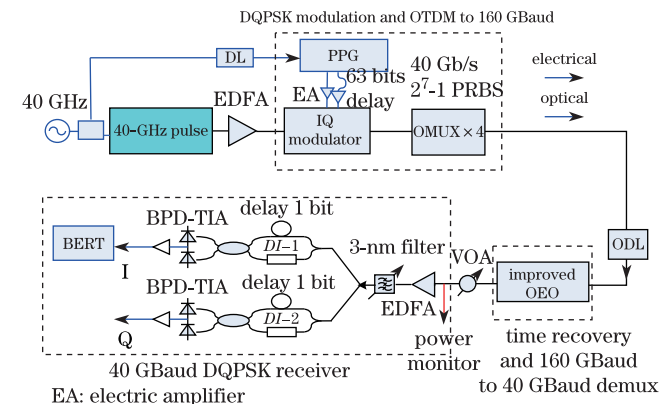


Fig. 4. Experimental setup of the 160-GBaud DQPSK OTDM demultiplexed to 40 Gbaud using the proposed OEO.

to serve as I and Q signals for the I/Q modulator. The modulated pulses are then passively multiplexed to 160 GBaud with a two-stage optical delay line. After time recovery and demultiplexing, the 40-GBaud signals pass by a variable optical attenuator, an erbium-doped fiber amplifier (EDFA) and a 3-nm BPF before sending to a delay-interferometer-based 40-Gb/s balanced receiver for bit error rate (BER) measurement.

Figure 5 shows the pulses generated from the cascaded MZM and PolM. These pulses have FWHM = 4 ps, ER = 20 dB, and SNR = 25 dB (measured by the OSO). The high SNR is attributed to the low insertion loss of PolM (2.1 dB), which is much smaller than the EAM (CIP 1550 nm) of approximately 10 dB.

The spectrum of the single sideband phase noise for the recovered 40-GHz clock signal using an electrical spectrum analyzer (Agilent N9030A PXA

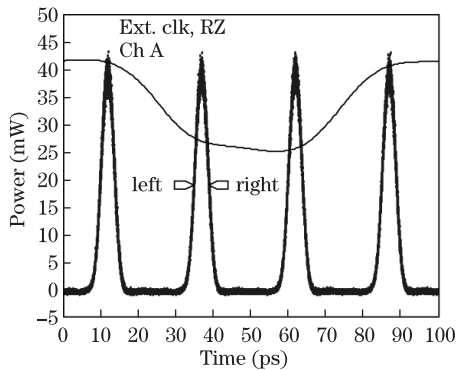


Fig. 5. Waveform of pulses generated from the cascaded MZM and PolM.

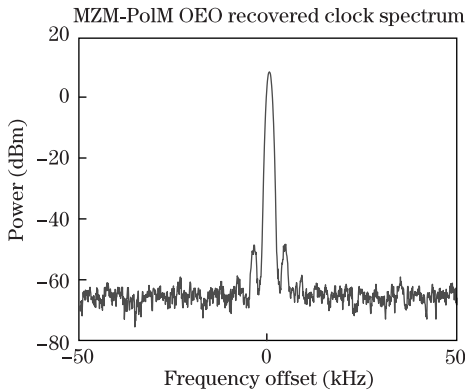


Fig. 6. (Color online) Spectrum of recovered 40-GHz clock.

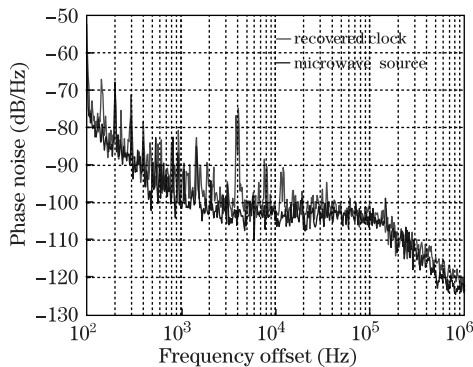


Fig. 7. (Color online) Measured phase noises of the recovered clock and microwave source.

Signal Analyzer) is shown in Figs. 6 and 7 (red line). The phase noise indicates a low timing jitter of 35 fs at 100 Hz to 1 MHz carrier offset for the recovered clock. Figure 7 (blue line) also plots the phase noise of the signal synthesizer as a reference. A small decrease in quality is observed in the recovered clock, except for the side mode, at approximately 3, 6, and 9 kHz offset introduced by the imperfect microwave amplifier.

Figure 8(a) shows the eye diagrams of the multiplexed 160-GBaud signals. By tuning the ODL before the improved OEO, each channel can be selected. After demultiplexing to 40 GBaud, Fig. 8(b) shows the waveforms of the four demultiplexed 40 GBaud tributaries. Figure 9 plots the BER curves of both I and Q tributaries for back-to-back (BTB) operation (without multiplexing/demultiplexing) and one of the demultiplexed 40-GBaud signals. For simplicity, only the curve with the worst BER performance among the four demultiplexed OTDM channels is shown because the four channels have similar BER performances. The BTB operation has a sensitivity (at BER =  $1 \times 10^{-9}$ ) of -28.4 dBm for both I and Q tributaries. For the worst case, the demultiplexed channel has sensitivities (at BER =  $1 \times 10^{-9}$ ) of -26.1 and -26 dBm for I and Q tributaries, respectively. The sensitivity penalty caused by the clock recovery and demultiplex is less than 2.4 dB.

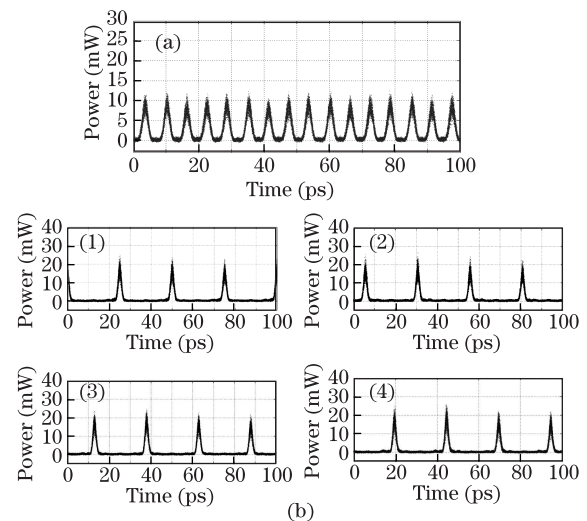


Fig. 8. (a) OTDM signals ( $4 \times 40$  GBaud), and (b) four tributaries demultiplexed by MZM PolM OEO.

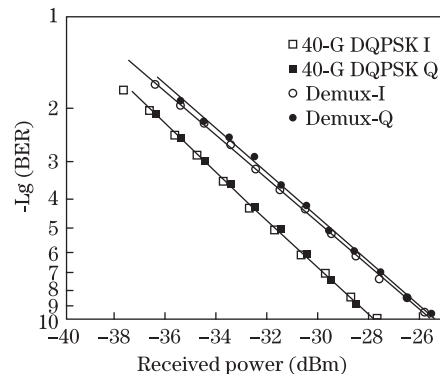


Fig. 9. BER for back-to-back operation and demultiplexed signal using the improved OEO.

In conclusion, we experimentally demonstrate an OEO based on cascaded MZM and PolM that realizes simultaneously clock recovery and demultiplexing without increased system complexity and cost. The timing jitter of the recovered clock signal is 35 fs. The scheme has the advantages of a significantly smaller loss than EAM. Error-free performance is achieved with the worst power penalty of 2.4 dB in demultiplexing 40 GBaud signals from 160-GBaud DQPSK signals using this scheme. Thus, this approach has potential applications in high-speed OTDM systems.

This work was partly supported by the National “863” Program of China (No. 2012AA011303), the National “973” Program of China (No. 2011CB301702), the National Natural Science Foundation of China (Nos. 61001121, 60932004, and 61006041), the Fundamental Research Funds for the Central Universities, and BUPT Excellent Ph.D. Students Foundation (No. CX201222).

## References

1. H. C. H. Mulvad, L. K. Oxenløwe, M. Galili, A. T. Clausen, L. Gruner-Nielsen, and P. Jeppesen, *Electron. Lett.* **45**, 280 (2009).
2. H. C. H. Mulvad, M. Galili, L. K. Oxenløwe, H. Hu, A. T. Clausen, J. B. Jensen, C. Peucheret, and P. Jeppesen, *Opt. Express* **18**, 1438 (2010).
3. F. Wang, X. Zhang, and E. Xu, *Opt. Laser Technol.* **43**, 1203 (2011).
4. S. Bauer, C. Bobbert, and G. Bramann, in *Proceedings of OFC'03* 105 (2003).
5. X. S. Yao and L. Maleki, *J. Opt. Soc. Am. B* **13**, 1725 (1996).
6. S. L. Jansen, M. Heid, and S. Spalter, *Electron. Lett.* **38**, 978 (2002).
7. H. Wang, D. Kong, and Y. Li, *Chin. Opt. Lett.* **10**, 040601 (2012).
8. M. D. Pelusi, *IEEE Photon. Technol. Lett.* **20**, 1060 (2008).
9. H. F. Chou, J. E. Bowers, and D. J. Blumenthal, *IEEE Photon. Technol. Lett.* **16**, 1564 (2004).
10. Y. Ji, Y. Li, J. Wu, B. B. Luo, Y. T. Dai, K. Xu, W. Li, X. B. Hong, and J. T. Lin, *IEEE Photon. Technol. Lett.* **24**, 772 (2012).
11. S. Pan and J. Yao, *J. Lightwave Technol.* **27**, 353 (2009).
12. H. Tsuchida, *J. Lightwave Technol.* **27**, 3777 (2009).
13. W. Zhou and G. Blasche, *IEEE Microwave Theory Techniques* **53**, 926 (2005).